2019 SECED Conference
Earthquake risk and engineering towards a resilient world
9-10 September 2019, Greenwich, London

EXPERIMENTAL AND NUMERICAL STUDY OF AN INNOVATIVE INTEGRATED SEISMIC AND ENERGY RETROFITTING SYSTEM FOR MASONRY WALLS USING TEXTILE REINFORCED MORTARS COMBINED WITH THERMAL INSULATION

Kyriakos KARLOS[1], Aristomenis TSANTILIS[2], Thanasis TRIANTAFILLOU[3]

Abstract: *Taking into consideration the seismic vulnerability of older buildings and the increasing need for reducing their carbon footprint and energy consumption, the application of an innovative system is proposed and investigated, which is based on the use of textile reinforced mortars (TRM) and thermal insulation as a means of combined seismic and energy retrofitting system of existing masonry walls. Medium scale tests were carried out on masonry walls subjected to out-of-plane and in-plane cyclic loading. The following parameters were investigated experimentally: one-sided versus two-sided insulation and/or TRM jacketing, placement of the TRM outside the insulation or in a sandwich form (over and under the insulation), as well as the displacement amplitude of the loading cycles. Additionally, numerical modeling was carried out, to predict the experimental results. From the results obtained in this study the authors believe that TRM jacketing may be combined effectively with thermal insulation, increasing the overall strength and energy efficiency of the masonry panels in buildings.*

Introduction

Masonry walls are prone to failure during high or moderate intensity earthquakes, hence they represent a significant hazard to life safety. Yet, structural decay due to ageing or cumulative seismic-induced damage poses a direct threat to the preservation and safeguarding of masonry structures that comprise an important part of many countries' cultural heritage. Hence, there is an urgent need for upgrading existing masonry structures, both in seismic areas, where structures designed according to old seismic codes have to meet upgraded performance levels demanded by current seismic design standards, and in non-seismic areas, e.g. due to change of usage and/or the introduction of more stringent design requirements.

Numerous techniques have been developed aiming at increasing the strength and/or deformation capacity of masonry walls. Textile reinforced mortar (TRM)-based solutions for masonry structures are becoming increasingly promising, as they combine the favorable properties offered by fiber reinforced polymer (FRP) systems (e.g. high strength and stiffness to weight ratio, high deformation capacity, corrosion resistance, ease and speed of application and minimal change in the geometry) while addressing most of the problems associated with the use of organic resins.

In addition to seismic retrofitting, given the high energy consumption associated to old buildings and their significant environmental impact, there is a strong need for effective solutions for the building envelope energy retrofitting. TRM jacketing has minimal, if any, thermal insulation capacity, while external or internal insulation has no load bearing capacity. In this study we propose the combination of the two systems into a single unit, which provides both seismic and energy retrofitting. In this new system, illustrated in Figure 1, the TRM is combined with the insulating material as a single unit, which may be either in the form of a prefabricated board or constructed in situ. Depending on the aesthetics and the constructability requirements, the system may be placed either on both sides of existing masonry walls or on one side. The TRM

[1]PhD Candidate, Univ. of Patras, Patras GR-26504, Greece, Email: karloskyriakos@gmail.com
[2]Civil Engineer, PhD, Univ. of Patras GR-26504, Greece
[3]Professor and Director of Structural Materials Lab., Dept. of Civil Engineering. Univ. of Patras, Patras GR-26504.

may be placed outside the insulating material, or inside, that is between the insulation and the masonry wall. All the above is investigated experimentally in the present study for the case of masonry walls subjected to in-plane or out-of-plane cyclic loading. More details for the case of out-of-plane and in-plane loading are given by Triantafillou et al. (2017) and Triantafillou et al. (2018), respectively. Moreover, the experimental results are found in good agreement with finite element modeling, which may be used in future studies to perform detailed parametric analyses. Further studies on the proposed technique are reported by Gkournelos et al. (2019).

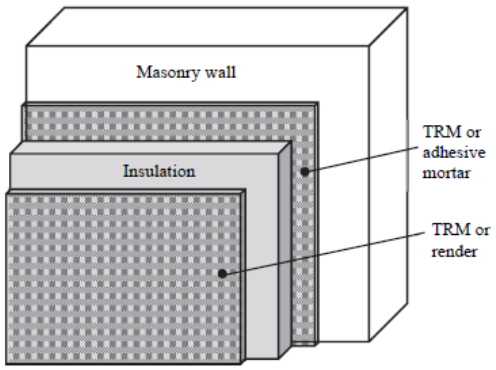

Figure 1. Schematic view of proposed structural and energy retrofitting system on one side of the masonry wall.

Experimental program

In-plane Loading

The investigation was carried out on three series of medium-scale, single-wythe, fired clay brick wallettes comprising running bond courses: (a) Series A ("shear walls") specimens (Figure 2a); (b) Series B ("beam-columns") specimens (Figure 2b); and Series C ("beams") (Figure 2c).

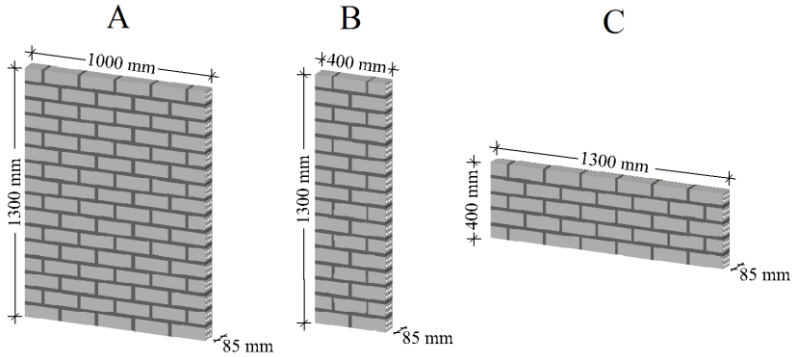

Figure 2. Geometry of (a) Series A, (b) Series B and (c) Series C specimens.

All specimens were subjected to cyclic in-plane loading, such that the plane of failure would form parallel to the bed joints for series A and B and perpendicular to the bed joints for Series C. The specimens were insulated using expanded polystyrene with strength of $\sigma_{u10\%}$=200 kPa (EPS200).

All specimens were constructed in the laboratory by an experienced mason using ridge-faced, 6-hole, horizontally perforated clay bricks (185x85x60 mm). The mean compressive strength of the walls in directions parallel and perpendicular to the bed joints was measured equal to 11 MPa and 3.71 MPa, respectively.

Whereas all specimens received the same amount of structural retrofitting (two layers of bidirectional textile with total weight 560 g/m^2) and the same amount of insulation (total thickness of insulation plates 40 mm), the investigation considered the following key parameters: one-sided versus two-sided insulation and TRM jacketing; placement of the TRM jackets outside the insulation or between the insulation and the masonry.

One specimen of each series was used as control, without TRM or insulation (Figure 3a). Each series included four different designs: (i) specimen i1M1i retrofitted on both sides with TRM

containing one layer of textile and 20 mm thick insulation plates applied externally on both sides (Figure 3b); (ii) specimen 1iMi1 retrofitted on both sides with TRM containing one layer of textile and 20 mm thick insulation plates applied on both sides between the TRM and the masonry (Figure 3c); (iii) specimen M2ii retrofitted on one side with TRM containing two layers of textile and two 20 mm thick insulation plates applied on the outside (on the same face with the TRM) (Figure 3d); and (iv) specimens Mii2 retrofitted on one side with TRM containing two layers of textile and two 20 cm thick insulation plates applied between the TRM and the masonry (Figure 3e).

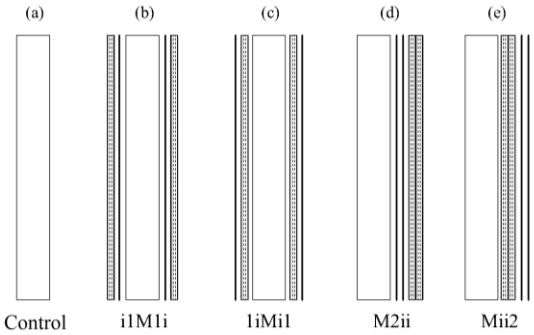

Figure 3. Specimens for in-plane loading: (a) Control; (b)-(e) retrofitted.

A total of 15 tests were performed (three series with five specimens in each series). The notation of specimens comprises a series of numbers and letters. The letter “A”, “B” or “C” at the beginning of the specimens’ notation denotes Series A, B or C respectively; the numbers (1 or 2) indicate the number of layers in the textile; “i" stands for a 20 mm thick insulation plate and “M” stands for masonry. Moreover, the sequence of numbers and letters represents the sequence of the different materials in each specimen.

Test set-up, Instrumentation and Procedure for In-plane Loading

All strengthened specimens were subjected to cyclic in-plane loading using a stiff steel frame. Series A specimens were tested as vertical cantilevers with a concentrated force at the top, at a distance of 1.18 m from the fixed base (Fig. 4a); Series B and C specimens were tested as horizontal beams in three-point bending, at a span of 1.15 m.

(a)

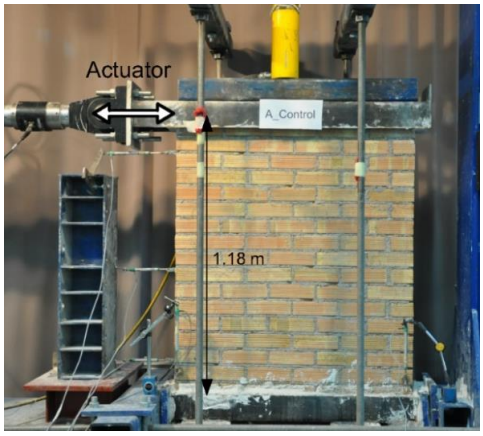

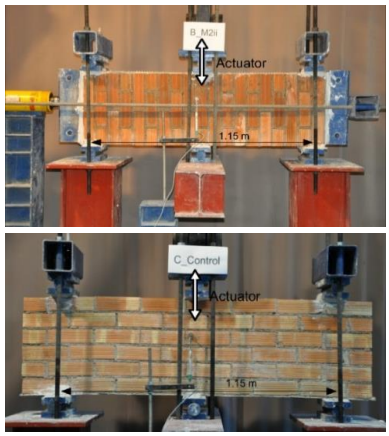

(b)

(c)

Figure 4. Experimental setup for specimens in: (a) Series A; (b) Series B; (c) Series C.

In addition to transverse loading, specimens in Series A and B were subjected to axial compression equal to 10% of the compressive strength. The axial load was applied using a hydraulic cylinder and a pair of threaded rods. Displacements were measured through the use of externally attached rectilinear displacement transducers.

Results and Discussion for In-plane Loading

The load versus displacement envelope curves for specimens in Series A, B and C are given in Figures 5 and 6. Typical photographs of failure mechanisms are given in Figures 7 and 8. Peak load values in the push or pull directions, P_{max}^{+}or P_{max}^{-}, displacements at failure, δ_u^{+} or δ_u^{-}, defined

as the point of the load versus displacement envelope curve where a 20% reduction in load was noted, cumulative energy dissipation capacity and observed failure modes are given in Table 1, for all specimens. The displacements recorded in Table 1 are those at piston position for specimens of Series A (as extrapolated by the displacement profile obtained from three horizontal displacement transducers), and at mid-span for specimens of Series B and C. In the load versus displacement plots, displacement values in the push direction, that is outward movement of the piston, are taken positive.

Specimen notation	**Peak load (kN)**		**Displacement at failure (mm)**		**Cumulative dissipated energy (kNmm) at:**		**Failure mode[a] (failure direction)**
	Push	**Pull**	**Push**	**Pull**			
Series A					cycle 5	cycle 10	
A_Control	19.9	17.3	>12	11.9	94.08	471.03	Rocking, toe crushing (pull)
A_i1M1i	31.5	30.5	12.0	11.0	139.31	622.68	FR (pull)
A_1iMi1	34.7	40.8	15.5	12.4	129.28	545.20	FR (pull)
A_M2ii	39.3	33.1	13.2	10.2	112.02	674.90	MC (pull)
A_Mii2	37.5	35.6	18.5	10.9	113.24	627.47	MC (pull)
Series B					cycle 3	cycle 7	
B_Control	20.0	24.0	6.0	6.1	31.06	345.54	Flexure (push)
B_i1M1i	37.1	32.6	8.3	7.0	28.59	355.11	FR (pull)
B_1iMi1	35.2	33.2	10.8	10.1	33.21	384.07	FR (pull)
B_M2ii	31.4	30.9	8.9	7.5	42.48	386.32	FR (pull)
B_Mii2	29.2	27.2	8.6	9.4	36.58	359.19	MC (push)
Series C					cycle 2	cycle 6	
C_Control	12.2	12.4	1.8	0.7	8.71	[b]	Flexure (pull)
C_i1M1i	33.9	18.9	6.2	4.8	5.77	267.01	FR (pull)
C_1iMi1	36.8	25.8	6.8	5.8	9.43	247.63	FR (pull)
C_M2ii	35.5	20.3	6.8	6.4	5.38	279.64	FR (pull)
C_Mii2	24.3	14.6[c]	8.4	10.3[c]	9.56	228.06	Combined in-plane and out-of-plane flexure (push)

Table 1. Summary of test results.

[a] FR = fiber rupture, MC = masonry crushing. [b] Failed in cycle 2. [c] Local crushing at one of the supports, hence these values should be used with caution.

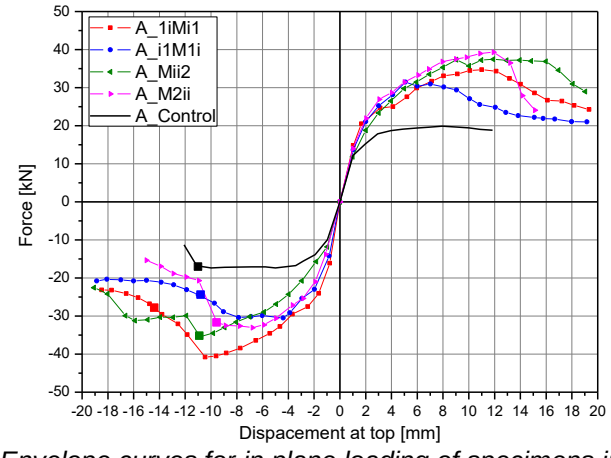

Figure 5. Envelope curves for in plane loading of specimens in Series A.

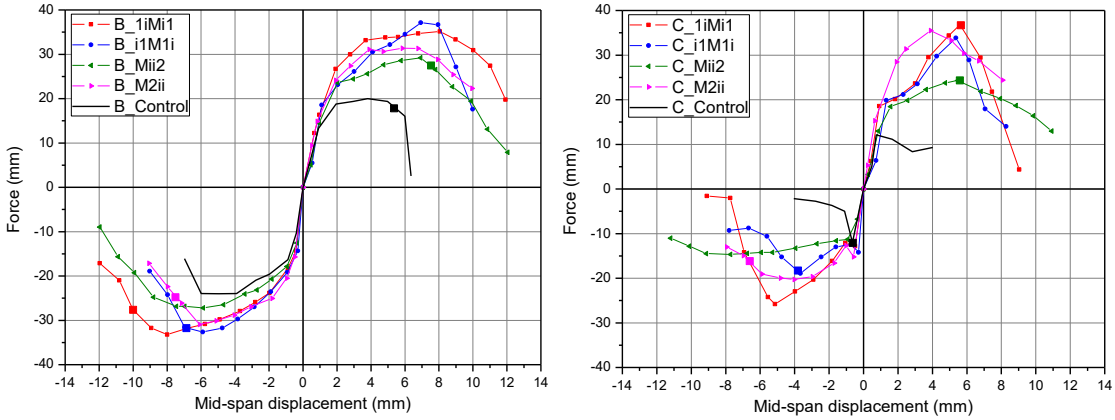

Figure 6. Envelope curves for in plane loading of specimens in Series B and C.

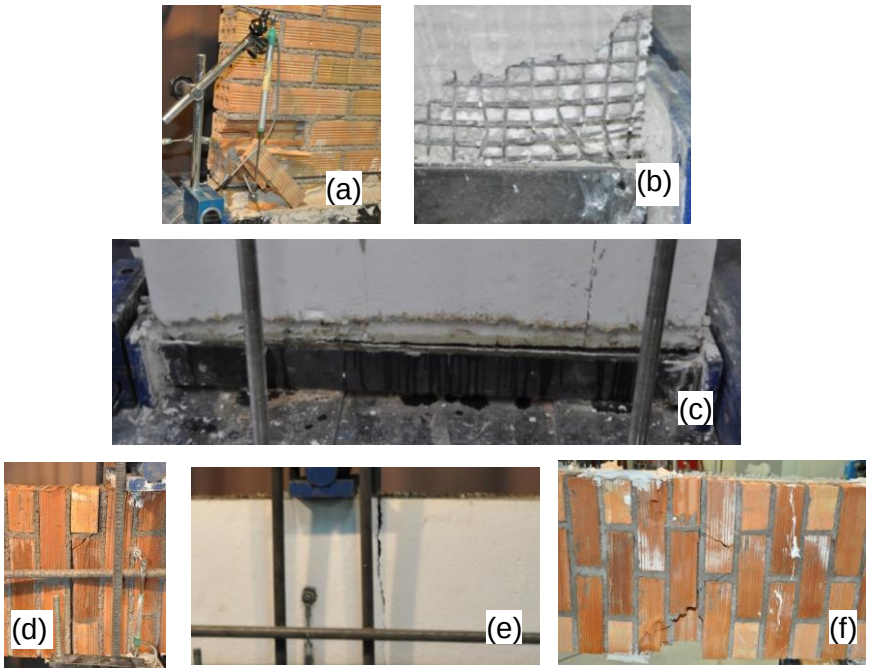

Figure 7. (a) Masonry toe crushing in specimen A_Control; (b) fiber rupture at the bottom part of A_1iMi1; (c) horizontal flexural crack at the bottom part of A_i1M1i; (d) Flexural cracking and crushing near the middle section of specimen B_Control; (e) flexural cracking and fiber rupture near the middle section of B_1iMi1, B_i1M1i and B_M2ii; (f) masonry crushing near the middle section of B_M2ii.

It is concluded that all retrofitted specimens (including the ones with insulation) failed at higher loads, had higher energy dissipation capacity and showed, in general, greater higher deformation capacity than unretrofitted masonry (Table 1). The increase in strength for retrofitted specimens was approximately: 60-100% in the push direction and 75-135% in the pull direction for the Series A; 45-85% in the push direction and 15-40% in the pull direction for Series B; 100-200% in the push direction and 55-110% in the pull direction for Series C. An important – yet not surprising – conclusion is that the exact positioning of the TRM and the insulating material does not play an important role in the in-plane response of retrofitted walls, as long as proper bonding between the different layers is achieved.

Out-of-plane Loading

A total number of 17 wall specimens were constructed using ridge-faced, 6-hole, horizontally perforated clay bricks, supplied by a local manufacturer, and a general-purpose masonry cement mortar. One specimen was used as control (M), without TRM or insulation (Figure 8a). Series D included six different designs: (i) specimens 2M2 and 2M2s retrofitted on both sides

with TRM containing two layers of textile and no insulation (Figure 8b); (ii) specimens 2iMi2 and 2iMi2s retrofitted on both sides with TRM containing two layers of textile and one layer of insulating material on both sides, between the TRM and the masonry (Figure 8c); (iii) specimens 1i1M1i1 and 1i1M1i1s retrofitted on both sides with TRM containing one layer of textile, one layer of insulating material and a second TRM jacket with one layer of textile, such that the TRM forms the faces of a sandwich system with the insulation as the core material (Figure 8d); (iv) specimens 2ii2M and 2ii2Ms retrofitted on one side with a sandwich system comprising TRM faces with two layers of textile and a core with two layers of insulation material (Figure 8e); (v) specimens 2iiM2 and 2iiM2s with two layers of insulation material on one side and TRM jackets with two layers of textile on the outside (Figure 8f); and (vi) specimen 2iMi2_na as in (ii) above (Figure 8c), but with retrofitting materials "non-anchored" (hence the letters "na" at the end of the specimens' notation), i.e. not extending all the way to the end of the walls, so that they were not clamped between the end supports and the masonry. All specimens in Series A, except the ones in design (vi), that is the one with "non-anchored" retrofitting, were tested in pairs, corresponding to two different displacement amplitudes (1 mm and 2 mm) of the loading cycles.

The notation of specimens in Series D comprises a series of numbers and letters. The numbers (1 or 2) indicate the number of layers in the textile, "i" stands for insulation and "M" stands for masonry. Moreover, the sequence of numbers and letters represents the sequence of the different materials in each specimen. The symbol "s" at the end of the specimens' notation denotes "small" displacement amplitude (1 mm). The control specimen is denoted as M (masonry only).

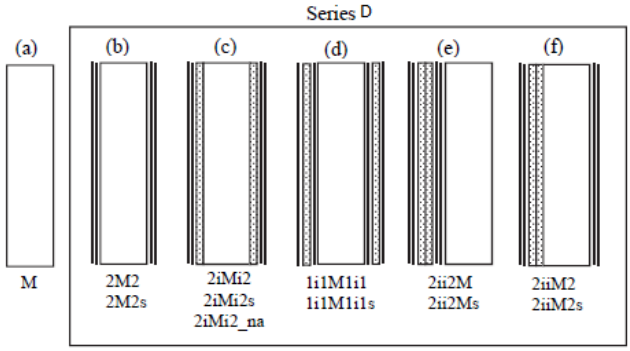

Figure 8. Specimens for out-of-plane loading: (a) Control; (b)-(f) Series A.

Test Set-up, Instrumentation and Procedure for Out-of-plane Loading

All strengthened specimens were subjected to cyclic out-of-plane loading using a stiff steel frame. The walls were laid horizontal (with the bonded surfaces facing upwards and downwards) and were loaded in three-point bending (Figure 9) at a span of 1.30 m. Two pairs of steel hinges were placed at each support (along the specimens' width, at top and bottom) and a third one was placed at mid-span (that is along the load application line).

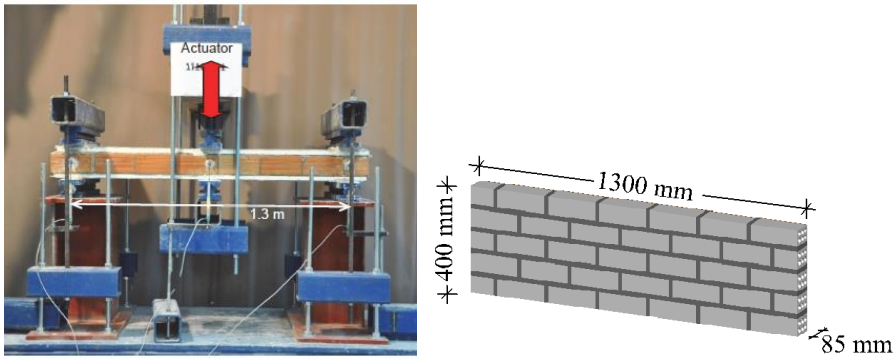

Figure 9. Experimental setup for out-of-plane testing.

All strengthened specimens were tested by applying the load in a quasi-static cyclic pattern of controlled displacements at a rate of 0.1 mm/sec. The loading sequence consisted of cycles at a series of progressively increasing displacement amplitudes in both directions (push and pull). The displacement amplitude increment was either 2 mm or 1 mm, as described above, and a single loading cycle was applied for each amplitude level.

Results and Discussion for Out of-plane Loading

The load versus displacement hysteresis loops for specimens in Series D are given in Figure 10. Typical photographs of failure mechanisms are given in Figure 11. Peak load values in the push and pull directions, $P_{max}^{+}$and P_{max}^{-}, mid-span displacements at failure, δ_u^{+} and δ_u^{-}, defined as the point of the load versus mid-span displacement envelope curve where either sudden load reduction was detected or a 20% reduction in load was noted in specimens with gradual post-peak load reduction, cumulative energy dissipation capacity and observed failure modes are given in Table 2, for all specimens.

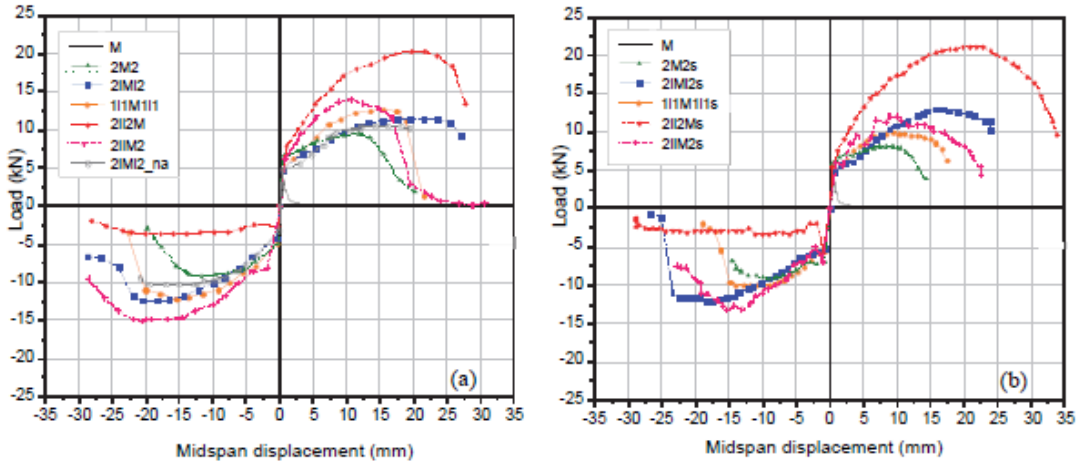

Figure 10. Envelope curves for out-of-plane loading: (a) 2 mm displacement increment; (b) 1 mm displacement increment.

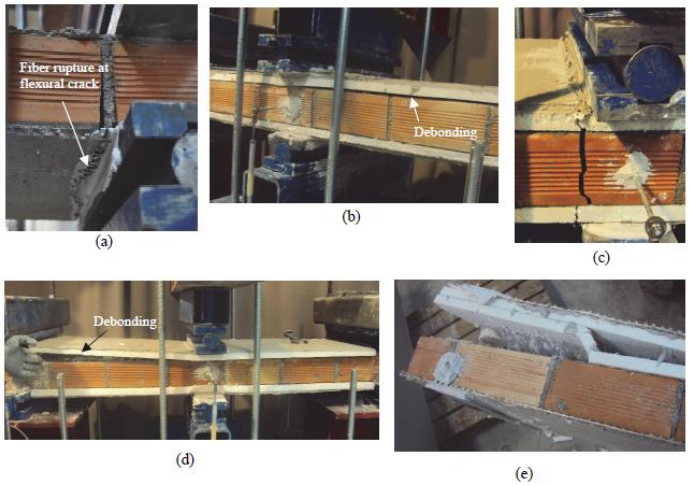

Figure 11. (a) Fiber rupture at mid-span; (b) debonding at the interface between the masonry and the insulation; (c) flexural cracking through the insulating material; (d) debonding, as a result of unfavourable anchorage conditions; and (e) debonding at the interface between the two insulation layers and between the masonry and the first insulation layer.

From the test results it is concluded that the proposed retrofitting system is highly effective. In terms of strength and deformation capacity, the combined use of TRM with insulation material is better than the use of TRM alone. TRM jacketing without insulation (specimen 2M2) increased the strength by approximately 170%, whereas this increase varied from 200% to 340% when the (double sided) textile reinforcement was combined with insulation layers, due to the

increased lever arm of the tension reinforcement. The respective numbers for specimens type "s" (small displacement amplitude increment) are 135%, 190% and 285%. As, expected, jackets with unfavourable bond conditions (specimen 2iMi2_na) were less effective; they increased the strength by at least 200%, whereas the strength increase in specimen 2iMi2, with favourable bond conditions, was at least 235%.

Specimen notation	**Peak load (kN)**		**Mid-span displacement at failure (mm)**		**Cumulative dissipated energy (kNmm) at cycle**		**Failure mode[b] (failure direction)**
Series D	**Push**	**Pull**	**Push**	**Pull**	**4 (8[a])**	**7 (14[a])**	
M	3.42	--	0.72	--	--	--	Flexural crack
2M2	9.28	9.28	13.78	15.69	154.29	421.19	FR[c] (both)
2iMi2	11.47	12.45	33.68	22.44	95.77	283.47	D[c] (push), FR (pull)
2iMi2_na	10.50	10.25	>28.23	27.48	80.23	221.12	D (pull)
1i1M1i1	12.70	12.21	19.66	20.17	104.80	326.91	FR (both)
2ii2M	20.26	3.66	25.97	24.20	75.06	250.09	FR (push), MC[c] (pull)
2iiM2	13.92	15.14	17.14	24.70	146.71	470.77	FR (push), D (pull)
2M2s	8.06	9.28	12.31	14.15	208.39	626.35	FR (both)
2iMi2s	12.97	12.17	23.49	23.49	144.79	461.72	FR (both)
1i1M1i1s	10.01	10.01	16.30	15.12	114.48	419.46	FR (both)
2ii2Ms	20.26	3.66	29.64	1.00	121.86	402.59	FR (push)
2iiM2s	11.96	13.18	17.26	18.91	194.51	657.37	FR (push), D (pull)

Table 2. Summary of test results for specimens in series D.

[a] For specimens tested at small displacement amplitude (1 mm)
[b] FR = fiber rupture, D = debonding, MC = masonry cracking.

In terms of deformation capacity, as expressed by the mid-span displacement at failure, TRM jacketing combined with thermal insulation was always much more effective than the TRM system alone, by up to approximately 140-145%.

Numerical modelling

Finite Elements Models

A numerical analysis was carried using finite elements, aiming to create a reliable and validated model to perform future parametric analyses. In order to simulate the experimental tests several 3D models were implemented using the Finite Element Code ANSYS release 14.5. More specifically, SOLID185 brick elements were used to simulate the masonry walls and the insulation panels, while SHELL181 shell elements were used for the TRM matrix. A total of ten models were constructed: five for in-plane loading of specimens in Series B and five for out-of-plane loading of specimens in Series D. The geometry of the models for each case considered and the element arrangement are presented in Figure 12. For simplicity both the masonry wall and the insulation panels were modelled assuming isotropic and homogeneous behaviour (macro model approach), while for the TRM tension only orthotropic membrane behaviour was adopted. Finally, steel plate brick elements (SOLID185) were introduced to simulate the boundary conditions at the loading points.

A multi-linear stress-strain constitutive relationship for masonry was adopted where the mechanical properties of control specimens were extracted from experimental data of masonry prisms in compression, assuming that tensile strength equal to 10% of the compressive. The control (M) model was calibrated in terms of the initial stiffness, which was fitted to the experimental results. For the TRM matrix a multi-linear material model was used, based on the experimental data of TRM coupons in tension, tested for different number of wythe layers and thicknesses according to each experimental group case, while for the insulation sheets also a nonlinear constitutive law, described as a closed cell foam material, was adopted with properties obtained from the manufacturer. Fully bonded interface conditions were assumed between the different materials. For time efficiency and computational convenience, a quarter or

a half of the whole specimen was simulated using the proper DOF constraints for symmetric conditions. A monotonically increasing vertical displacement was prescribed at the middle nodes.

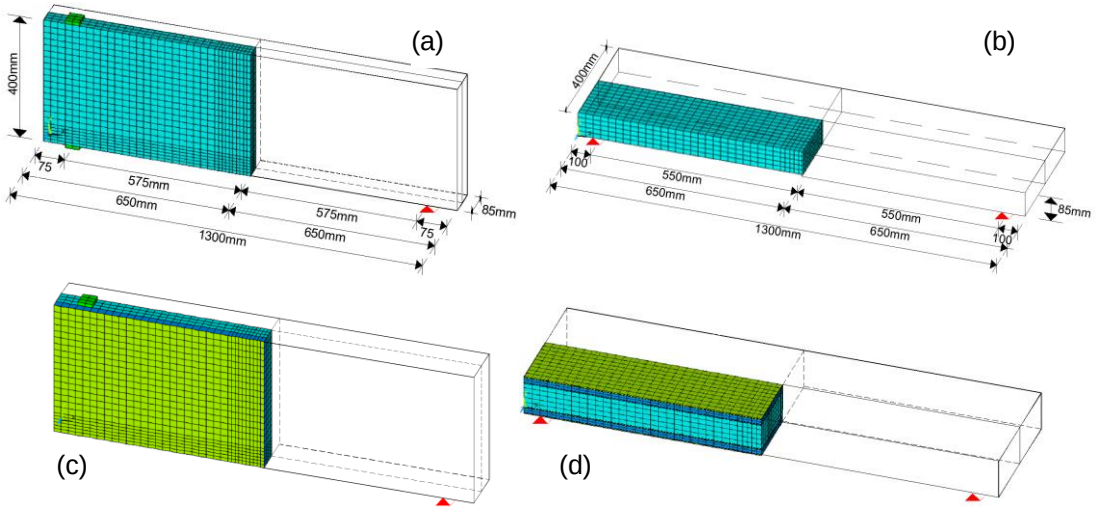

Figure 12. Schematic arrangement and geometry of control specimens: (a) in-plane model, Series B ("beam-columns"), (b) out-of-plane model, Series D-"s". View of model for (c) Specimen 1iMi1 for in-plane loading and (d) Specimen 2iMi2 for out-of-plane loading.

Numerical Results and Discussion

Plots of the force-displacement envelope curves for the in-plane (Series B) and out-of-plane (Series D-"s") loaded specimens versus the numerical predictions are presented in Figures 13 and 14. Overall, the results show good agreement with the experimental data, indicating that the numerical analysis is capable of reproducing the observed behaviour with the exception of the post-peak reduction of strength due to restraints of the program to simulate stress-strain curves with sharp negative slopes. All retrofitted specimens exhibited an increase of their strength compared to the control ones, in both groups.

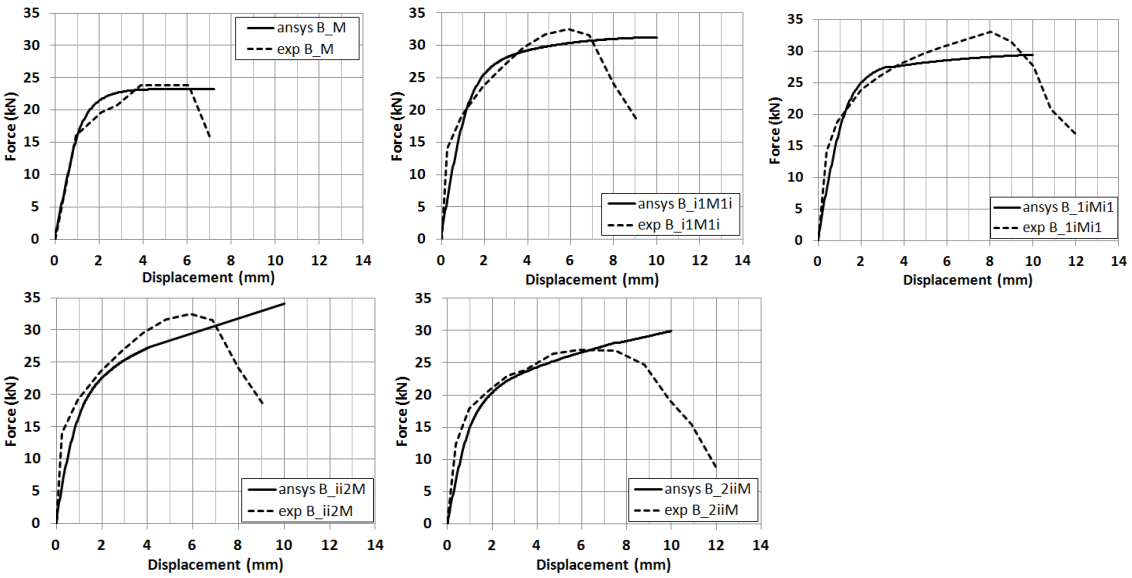

Figure 13. Experimental versus numerical results for the in-plane loaded specimens.

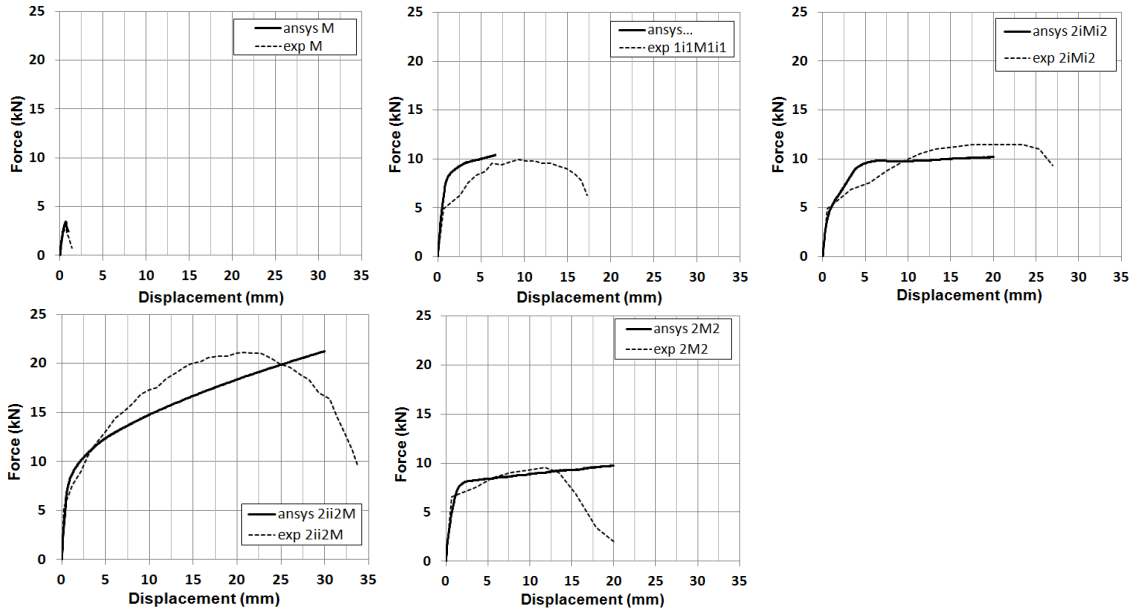

Figure 14. Experimental versus numerical results for the out-of-plane loaded specimens.

Conclusions

The present study presents an innovative system for both seismic and energy retrofitting of masonry walls, involving the combination of TRM and thermal insulating materials. The system was tested on brick masonry wallettes subjected to in-plane and out-of-plane cyclic loading.

Overall, it is concluded that the new retrofitting system not only improves the thermal performance of masonry walls but also is highly effective as a means of seismic retrofitting for out-of-plane and in-plane loading, as long as proper bonding between the different layers is achieved. According to the experimental results, the exact positioning of the TRM and the insulating material does not play an important role in the in-plane response of retrofitted walls. On the other hand, in out-of-plane loading, positioning the reinforcement outside the thermal insulation improves substantially the strength and deformation capacity when compared to TRM jacketing alone.

Finally, the FE analysis yielded good agreement with the experimental results, hence it can be used for future parametric studies or in larger and more realistic case studies.

Acknowledgements

The experimental data have been obtained with assistance from E. Argyropoulou, L. Georgiou, P. Kapsalis and K. Kefalou.

References

Gkournelos PD, Bournas DA, Triantafillou TC (2019). Combined seismic and energy upgrading of existing reinforced concrete buildings using TRM jacketing and thermal insulation, *Earthquakes and Structures*, in press.

Triantafillou TC, Karlos K, Kefalou K, Argyropoulou E (2017a). An innovative structural and energy retrofitting system for URM walls using textile reinforced mortars combined with thermal insulation: Mechanical and fire behavior, *Construction and Building Materials*, 133, 1-13.

Triantafillou TC, Karlos K, Kapsalis P, Georgiou L (2018). Innovative structural and energy retrofitting system for URM walls using textile reinforced mortars combined with thermal insulation: Mechanical and fire behavior", *Journal of Composites for Construction*, 22(5), 04018029, doi 10.1061/(ASCE)CC.1943-5614.0000869.

ANSYS ® Academic Research, Release 14.5.